Using Accelerated Pavement Testing to Study Asphalt Aging and Embrittlement

X. Qi
SES Group / Turner-Fairbank Highway Research Center, McLean, Virginia, USA

N. Gibson
Federal Highway Administration, McLean, Virginia, USA

A. Andriescu
SES Group / Turner-Fairbank Highway Research Center, McLean, Virginia, USA

J. Youtcheff
Federal Highway Administration, McLean, Virginia, USA

ABSTRACT: Seven pavement sections with both unmodified and modified asphalt binders at the Federal Highway Administration (FHWA) pavement test facility were loaded at two different conditions: 21 months after construction and 62 months after construction plus accelerated aging. The accelerated aging process heated the full scale pavements to 74°C for eight weeks. The fatigue performance data obtained under these two distinctive conditions enables the study of aging and embrittlement process for different types of asphalt binders. Accelerated aging significantly decreased the fatigue performance while keeping the overall ranking of before and after aging. Two exceptions were the Arizona crumb rubber mixture which was significantly impacted by the aging process and the reacted terpolymer HMA which was largely un-affected by the aging process. The aged sections exhibited a mixture of top-down and bottom-up fatigue cracking. IDT $|E^*|$ data from field cores indicate that the largest increase in mixture stiffness was due to more than five years of natural exposure while the accelerated-aging process did not result in a significant stiffness increase. Extracted binder stiffnesses were characterized from the upper 25mm HMA. The effect of aging process was more significant at intermediate temperatures than at high temperatures. Natural exposure aging (62 months) was equivalent to more than the standard 20 hours in the Pressure Aging Vessel. Research continues on extracted binders obtained from all of the accelerated-aged lanes; candidate parameters to replace the Superpave fatigue cracking specification will be compared back to the accelerated-aged performance in addition to the early-aged fatigue cracking performance.

KEY WORDS: Accelerated pavement testing, fatigue cracking, asphalt aging.

1 INTRODUCTION & BACKGROUND

In the summer of 2002, the Federal Highway Administration (FHWA) initiated a transportation pooled fund study TPF-5(019) to validate and refine changes proposed in the Superpave binder specification to properly grade modified binders. An important part of this research effort was using accelerated pavement testing (APT) to identify candidates to replace

the Superpave asphalt binder fatigue cracking specification parameter. This parameter is currently the linear viscoelastic loss modulus, $|G^*|\times\sin\delta$, and research has shown its ability to discriminate fatigue cracking performance to be questionable (Bahia et al. 2001). Seven lanes of pavements constructed with both unmodified and modified binders at FHWA's pavement test facility were loaded with two accelerated loading facilities (ALF) to achieve this research objective.   All these seven lanes of pavements were designed to have the same pavement structure and materials except for the variation in binders so that the relationship between pavement fatigue performance and binder fatigue parameter can be established. The pavement structure contains a 100 mm hot mix asphalt (HMA) layer placed on top of a crushed aggregate base (CAB) over a relatively stiff AASHTO A-4 subgrade (decomposed bedrock). The total thickness of the HMA and CAB layers is 660 mm. The HMA mix design for the test lanes was an identical, dense, coarse graded 12.5 mm nominal maximum aggregate mix and binder type was varied. Asphalt binders included were an unmodified control (Lane 2), unmodified air blown (Lane 3), a terminally blended crumb rubber (CR-TB) (Lane 5), styrene-butadiene-styrene (SBS) (Lane 4), and reacted terpolymer (Elvaloy) (Lane 6). Lane 7 utilized the unmodified control mixture with 0.3% polyester fiber by weight of aggregate. Lane 1 was a composite pavement having the unmodified control mixture on the bottom with an Arizona type gap-graded, wet-process crumb rubber modified asphalt mix (CR-AZ) on top. Details of the structural configuration and materials in the APT experiment are described in literature (Kutay et al. 2008).

One caveat of asphalt pavements in APT experiments is that loading takes place in the early stages of life. This is considered favorable for rutting, but less so for fatigue cracking experiments. Fatigue failure is not expected to be an early age phenomenon for in-service pavements. To capture the effects of pavement aging and embrittlement on fatigue failure, seven pavement test sections received an intense, in-situ accelerated aging process after more than five years of natural exposure. All these seven lanes of pavements were loaded at two different conditions: 21 months after construction and 62 months after construction plus accelerated aging. Therefore, full-scale fatigue cracking performance data obtained from the distinctive early-aged and accelerated-aged conditions allows the aging and embrittlement process in different types of modified and unmodified asphalt binders to be studied. The objective of this paper is to quantify the impact of aging on full-scale fatigue cracking. In addition, in-situ changes in HMA dynamic modulus $|E^*|$ and rheological properties of extracted asphalt binder are summarized from ALF lanes with data available at the time.

2 FULL-SCALE AGING AND LOADING CONDITIONS

ALF machines simulate traffic with controlled loading and pavement temperatures using 29 meter long frames with rails to direct a single, half-axle loaded between 33 to 84 kN. Each machine is capable of applying an average of 35,000 wheel passes per week. Both, early-aged and accelerated-aged fatigue loading was conducted at 19°C using pre-programmed transverse wander (+/- 133 mm standard deviation) and a 425 super-single tire inflated to 827 kPa loaded at 74 kN. Periodically during the fatigue tests, the ALF was stopped and cracks were manually traced onto clear plastic Mylar sheets as they formed at the surface of the pavements. Different color pens were used to correspond to the number of load repetitions. Measured fatigue cracking was quantified by the percentage of area cracked.

Fatigue testing began on the early-aged 100 mm HMA sections 21 months (on average) after construction and required 11 months (on average) to complete. Accelerated aging began on the pavements 62 months (on average) after construction. Until this time, the test sections were undisturbed, unloaded and exposed to the natural environment while fatigue loading

progressed on a separate set of thicker 150 mm HMA lanes in the experiment. Accelerated aging was completed using the same radiant heaters used to control the temperature at 19°C. Wheel loads were not applied during accelerated aging. Thermocouples were embedded at various depths and the pavements were heated to 74°C, which is the highest practical temperature the radiant heaters under the ALF could achieve. Thermocouples embedded at a 20 mm depth were used in a closed loop with temperature controllers to maintain the pavement temperature. The average and standard deviation of the surface temperature was 74.8^{o}C and 1.3^{o}C. The average and standard deviation of the HMA bottom temperature was 73.7^{o}C and 1.5^{o}C. Although the influence of solar radiation on asphalt binders has been known for some considerable time, the influence of ultraviolet (UV) light on asphalt aging was not included in the scope of this study due to the fact that UV rediation only affects the very upper layers of the pavement surfacing (Airey G. 2003).

3 RESULTS

3.1 Full-Scale Fatigue Performance

Figure 1 graphically presents the early-aged and accelerated-aged fatigue results in terms of percent surface area cracked versus ALF loading passes. The legend indicates the designated lane/site and pavement aging condition. For example, L2S3 refers to Lane 2 Site 3 before accelerated aging and L2S4 (Aged) refers to as Lane 2 Site 4 tested after accelerated aging. Asphalt aging and embrittlement significantly reduces fatigue life.
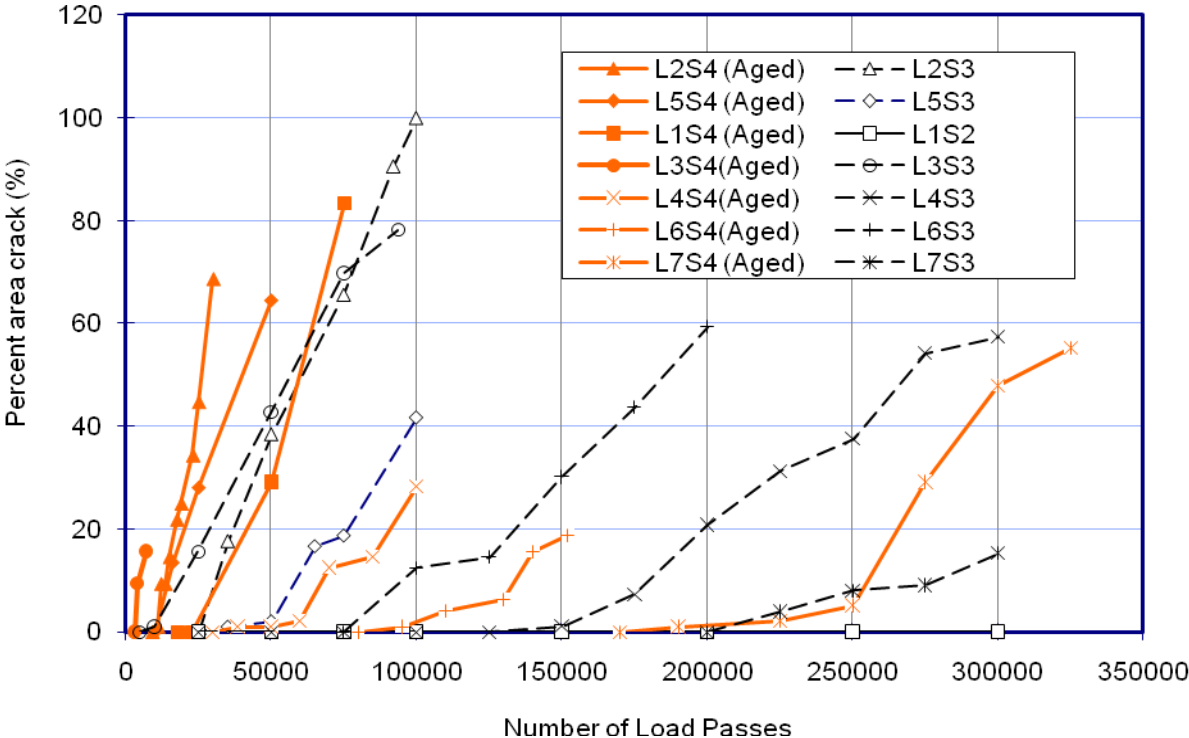
Figure 1: Pavement surface percent area crack versus ALF loading pass.

Table 1 quantifies the effect of aging and embrittlement on pavement fatigue resistance. The ALF load passes to surface crack initiation and passes to 15% surface cracking for the early-aged and accelerated-aged conditions are summarized. The ratio between early-aged (EA) and accelerated-aged (AA) ALF passes is provided as well. A larger ratio means aging

had a greater influence on the fatigue resistance, but does not necessarily indicate better or worse performance relative to other mixtures. It is observed that pavements tested at the early-aged condition showed better fatigue resistance than those tested at the accelerated-aged condition for all but one of the seven lanes. The exception is Lane 6 with reacted terpolymer binder that showed equal or potentially slightly better performance than early-aged.

Table 1: Summary of ALF passes at surface crack initiation and 15% cracking.

Lane Number	Binder Type	ALF pass at surface crack initiation			ALF pass at 15% surface cracked		
		EA	AA	EA/AA	EA	AA	EA/AA
1	CR-AZ	>300000	23,000	>13.0	>300000	36,000	>8.3
2	PG 70-22	35,000	11,000	3.2	34,000	15,000	2.3
3	Air-Blown	10,000	4,000	2.5	24,500	6,500	3.8
4	SBS LG	150,000	38,000	3.9	190,000	85,000	2.2
5	CR-TB	26,000	16,000	1.6	64,000	17,000	3.8
6	Terpolymer	100,000	95,000	1.1	125,000	135,000	0.9
7	Fiber	225,000	190,000	1.2	300,000	260,000	1.2

EA = Early-aged, AA = Accelerated-aged.

Figure 2(a) contains X-ray computed tomography and photographs of cores from the early-aged sections that confirms the type of cracking was classical, bottom-up (alligator) fatigue. Figure 2(b) is a photograph of a core from the composite pavement in Lane 1 that shows a typical bottom-up fatigue crack that propagated through the bottom control HMA layer and was arrested at the Arizona gap-graded crumb rubber HMA. A series of cores were
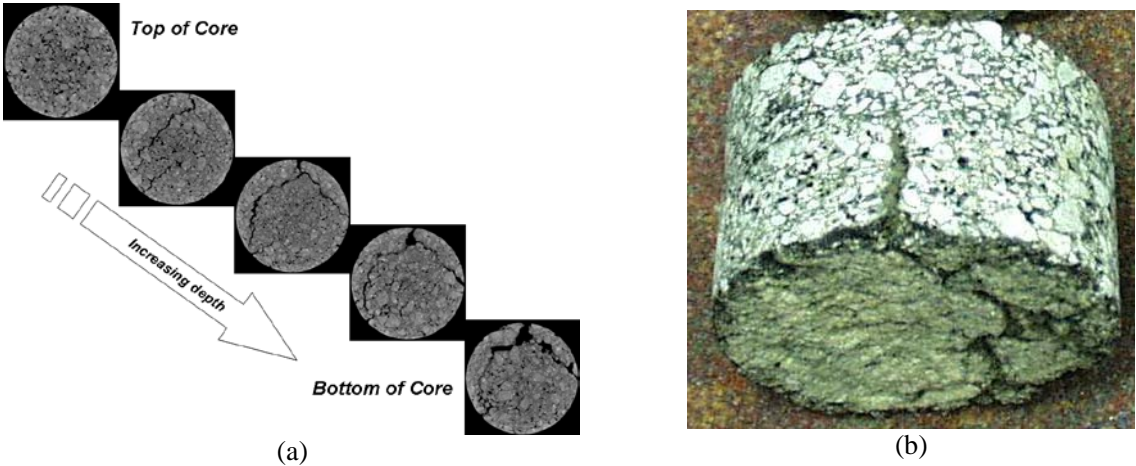
Figure 2: Bottom-up fatigue cracking; (a) X-Ray computed tomography images of ALF core showing crack propagating from bottom to top (b) Bottom-up fatigue cracking arrested at Arizona gap graded crumb rubber mix.

taken from the accelerated-aged sections after fatigue loading to determine if aging caused a different type of fatigue cracking. The sides of the cores were examined for the presence of cracks propagating from the top-down or from the bottom-up and full depth cracks. Aging due to natural exposure plus accelerated means has triggered a combination of top-down and bottom-up fatigue cracks. Table 2 quantifies the types of cracks observed with the majority

type highlighted in grey. Three of the five lanes with available data exhibited predominately top-down cracking and one lane had a majority of bottom-up cracking. The Air Blown lane which cracked very fast had mostly cracked through and some could have been top-down or bottom-up. Figure 3 provides some qualitative photographs showing both top-down and bottom-up fatigue cracks observed in the aged test sections.

Table 2: Assessment of bottom-up and top-down cracking in aged test sections.

	Total Counts	Bottom-up Cracks		Top-Down Cracks		Full-Depth Cracks	
		Counts	Percentage	Counts	Percentage	Counts	Percentage
Lane 1 CR-AZ/Control	15	3	20%	11	73%	1	7%
Lane 2 Control	6	0	-	5	83%	1	17%
Lane 3 Air Blown	5	1	20%	0	-	4	80%
Lane 5 CR-TB	18	10	56%	5	28%	3	17%
Lane 6 Reacted Terpolymer	13	5	38%	8	62%	0	-

Figure 3: Top-down and bottom-up fatigue cracks in aged test sections (Lane 5 CR-TB).

3.2 Pavement Core Dynamic Modulus |*E**|

Cores were cut before and periodically during the first four weeks of the eight-week accelerated aging period. Cores were taken from the ALF lanes at week 0 that represents more than five years of natural exposure but no accelerated-aging. Cores were then taken at one week, two weeks, three weeks and four weeks during the full-scale accelerated aging period. Pairs of cores were taken at each point in time. One core was sampled from locations on the west side of the loaded area and the other core was sampled on the east side. The 150 mm diameter cores were taken 180 mm from the outer bounds of the lateral wheel wander, but this location was still well within the area heated for accelerated aging. The core holes were filled with patching material, and then surfaces sealed with crack sealant. Coring did not influence the fatigue crack pattern that developed. The cores were split at the construction lift boundary and each lift was approximately 50 mm thick. The air void content was measured on the top lift and bottom lift cores using the saturated surface dry technique (AASHTO T-166).

The 150 mm diameter x 50 mm thick cores were measured for dynamic modulus |E*| at +19°C and -19°C in the indirect tension mode (IDT) rather than the typical axial compression mode on cylindrical samples. The IDT |E*| methodology developed by Kim et al (2004) was followed. The frequencies used at each temperature were 10 Hz, 5 Hz, 1 Hz, 0.5 Hz and 0.1 Hz. Temperatures warmer than +19°C were not used to avoid damaging the test specimens. A full set of IDT |E*| data from weeks 0, 1, 2, 3 and 4 was available only for Lane 4 SBS-LG and Lane 7 Fiber. These data are plotted in Figure 4 and Figure 5. In each figure, the dynamic

modulus master curve from lab-produced samples at 7% air voids generated from data between 4°C and 58°C is shown in solid grey. The lab-produced samples underwent short-term aging (AASHTO R-30). The average air void content from the top lift and bottom lift of Lane 4 SBS-LG was 7.8% and 5.4%, respectively. The average air void content from the top lift and bottom lift of Lane 7 Fiber was 7.9% and 7.8% respectively. The higher density in the lower lifts is reasonable since additional compaction may have occurred in the lower lift after the top was placed and compacted. +19°C is the reference temperature for both the field cores and the lab produced samples. The -19°C data were shifted using extrapolations of the time-temperature shift function from lab-produced $|E^*|$ master curves. Triangular data points are used to represent the IDT $|E^*|$ data from the top lifts and circular data points are used to represent the IDT $|E^*|$ data from the bottom lifts. Different shades of grey-scale from white to black indicate when the core was taken during the accelerated aging.

It is clear from the +19°C data that the top lift cores are notably stiffer than the bottom lift cores despite having a higher air void content. On the other hand, this trend does not appear to be as clear at -19°C. At both temperatures and depths there does not appear to be a clear trend of increasing stiffness as the time of accelerated aging accumulated. Inherent replicate-to-replicate variability could be masking this effect. The data also indicate that the largest increase in stiffness occurs due to more than five years of natural exposure and little else can be detected using IDT $|E^*|$ to assess changes in stiffness due to accelerated aging over a four week period.

3.3 Extracted Binder DSR measurements

The IDT $|E^*|$ properties of the bulk HMA mixture showed no clear trend of stiffness increase with cumulative time under accelerated aging, but binder properties exhibit significantly less replicate-to-replicate variability than HMA mixtures. After IDT $|E^*|$ testing, the top lift cores were further trimmed in half yielding a "top-top" layer representing the upper 25 mm of the
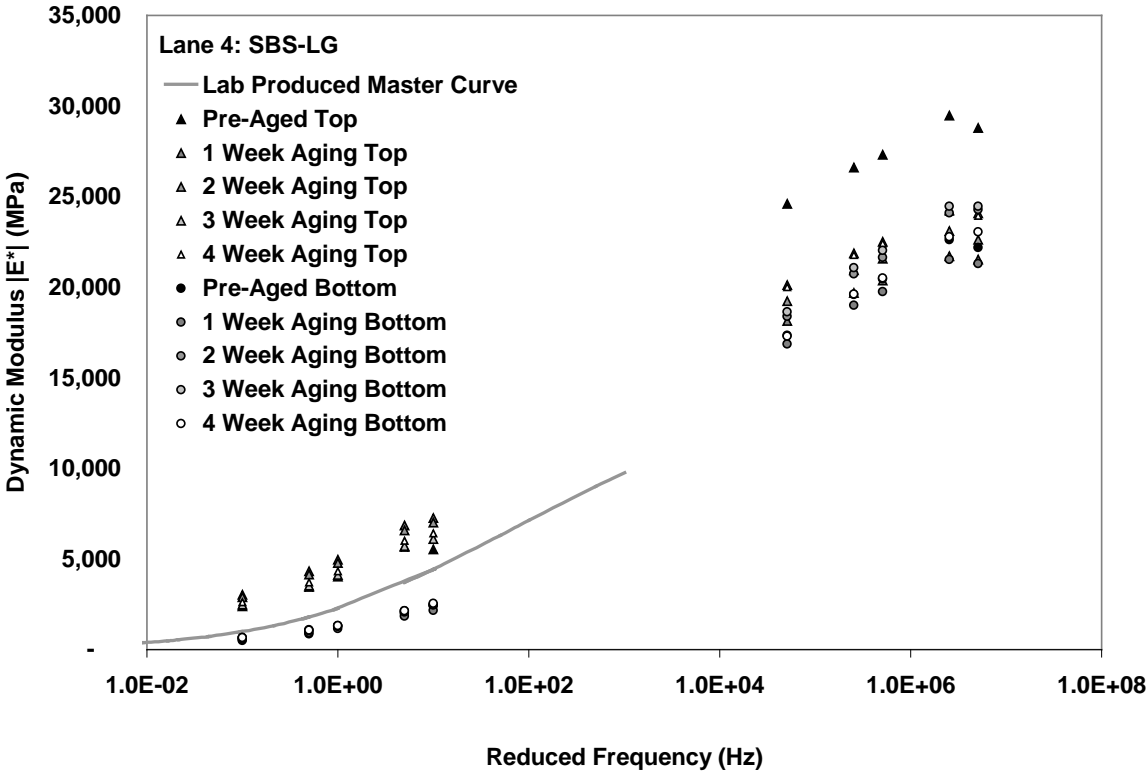
Figure 4: Lane 4 SBS-LG mix, indirect tension test (IDT) dynamic modulus $|E^*|$.
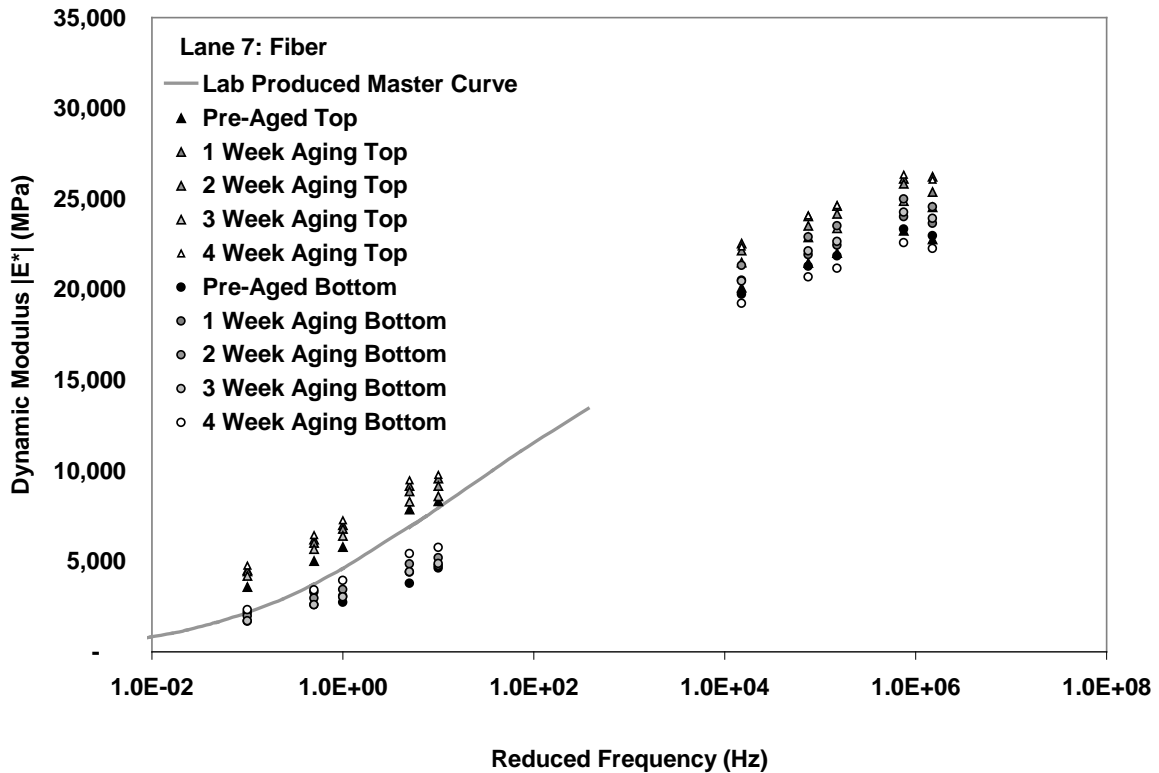
Figure 5: Lane 7 fiber mix, indirect tension test (IDT) dynamic modulus |E*|.

top lift. The asphalt binder was extracted, recovered and tested from the extremes at week 0 and week 4. In addition, original binders stored in cans were retested under a series of laboratory accelerated-aged conditions to develop a sequential aging profile. The aging sequence included the following conditions: original (no aging), standard aging through the Rolling Thin Film Oven (RTFO, AASHTO T-240), and Pressure Aging Vessel (PAV, AASHTO R-28) over a period of 5, 10, 20, 30, 40, 60, and 80 hours. 20 hours is the standard PAV duration. The rheological properties of the recovered binders from the full-scale accelerated aged sections are then placed within the aging sequence profile to determine how laboratory accelerated aging and full-scale natural and accelerated aging compare to one another. The extracted and laboratory aged binders were tested in a dynamic shear rheometer (DSR) for the dynamic modulus $|G*|$ and phase angle δ at an intermediate temperature of $19^{o}C$ and a high temperature of $76^{o}C$. The high temperature rutting parameters $|G*|/\sin\delta$ was calculated from $76^{o}C$ data shown in Table 3 and the intermediate temperature fatigue parameter $|G*| \times \sin\delta$ was calculated from $19^{o}C$ data shown in Table 4. A full set of data is available for three test sections: Lane 2 unmodified control, Lane 3 unmodified air blown and Lane 4 SBS modified asphalts.

The data indicate that both greater than five years of natural exposure and accelerated-aging is equivalent to different aging conditions depending on the type of binder and the temperature it is being characterized. Aging due to natural exposure over more than five years in the top 25mm of HMA is equivalent to greater than the standard 20 hours in the PAV for both unmodified and polymer modified binders. The exception was for the high temperature properties of the SBS polymer modified binder, which were between 10 hour and the standard 20 hour PAV duration. The effect of both natural aging exposure and accelerated aging was more severe based on the intermediate binder rheological properties; between twice to four times the standard duration in the PAV. Full-scale accelerated aging was successful in

Table 3: Core extracted and laboratory aged high temperature binder properties.

Lane 2 Control $|G^*|/\sin\delta$ 76°C (kPa)		Lane 3 Air Blown $|G^*|/\sin\delta$ 76°C (kPa)		Lane 4 SBS-LG $|G^*|/\sin\delta$ 76°C (kPa)	
Original	0.7	Original	1.02	Original	0.99
RTFO	1.4	RTFO	2.48	RTFO	1.86
PAV 5 Hour	2.5	PAV 5 Hour	4.25	PAV 5 Hour	3.27
PAV 10 Hour	3.4	PAV 10 Hour	4.54	PAV 10 Hour	4.06
PAV 20 Hour	*5.3*	*PAV 20 Hour*	*7.90*	Field Pre Aged	5.32
PAV 30 Hour	6.7	PAV 30 Hour	10.70	Field 4 Weeks	5.99
PAV 40 Hour	11.4	Field Pre Aged	17.27	*PAV 20 Hour*	*7.48*
Field Pre Aged	16.7	PAV 40 Hour	18.47	PAV 30 Hour	8.20
PAV 60 Hour	17.7	Field 4 Weeks	41.63	PAV 40 Hour	13.89
PAV 80 Hour	35.6	PAV 60 Hour	50.52	PAV 60 Hour	31.17
Field 4 Weeks	44.1	PAV 80 Hour	53.67	PAV 80 Hour	38.51

Table 4: Core extracted and laboratory aged intermediate temperature binder properties.

Lane 2 Control $|G^*|\sin\delta$ 19°C (kPa)		Lane 3 Air Blown $|G^*|\sin\delta$ 19°C (kPa)		Lane 4 SBS-LG $|G^*|\sin\delta$ 19°C (kPa)	
RTFO	2,971	Original	1,214	Original	1,011
Original	3,207	RTFO	2,072	RTFO	1,950
PAV 5 Hour	4,873	PAV 5 Hour	3,997	PAV 5 Hour	2,449
PAV 10 Hour	7,819	PAV 10 Hour	4,417	PAV 10 Hour	2,637
PAV 20 Hour	*9,013*	*PAV 20 Hour*	*5,530*	*PAV 20 Hour*	*3,209*
PAV 30 Hour	10,027	PAV 30 Hour	6,154	PAV 30 Hour	4,106
PAV 40 Hour	11,107	PAV 40 Hour	6,847	PAV 40 Hour	4,275
PAV 60 Hour	12,960	Field Pre Aged	6,890	PAV 60 Hour	4,870
PAV 80 Hour	12,688	PAV 60 Hour	8,034	PAV 80 Hour	6,875
Field Pre Aged	16,024	PAV 80 Hour	8,898	Field 4 Weeks	8,680
Field 4 Weeks	18,292	Field 4 Weeks	9,677	Field Pre Aged	8,774

significantly altering the in-situ binder properties beyond more than five years of natural exposure in the top 25 mm of HMA.

4 ONGOING ACTIVITIES

Table 5 summarizes the ranking observed between early-age, full-scale Accelerated Load Facility fatigue cracking, lab-scale viscoelastic continuum damage (VECD) fatigue tests (Kutay et al. 2008) and an assortment of alternative binder test methods (Shenoy 2002, Bodley et al. 2007, Martono and Bahia 2008, Andriescu et al. 2009, Johnson et al. 2009). The Kendall's tau rank order parameter (Kendall and Gibbons 1996) was utilized to compare the strength of different binder parameters to discriminate fatigue and cracking performance. Kendall's tau was chosen rather than the coefficient of determination, R^2, since this parameter must be taken with caution when calculated from a relatively small data set. Kendall's tau can be calculated from small or large data sets and ranges between -1 and +1. Negative scores do not necessarily mean the parameter is incorrect. Values closer to zero indicate worse ranking while values closer to +1 or -1 indicate better quality ranking. Positive ranking scores are correct for expected proportional trends such as number of cycles to binder fatigue failure ranked against number of cycles to ALF cracking. Negative scores would be correct for expected inverse trends such as limiting binder modulus (i.e. loss modulus) ranked against number of cycles to fatigue failure. The direction of association for all of the binder

parameters is correct except the binder stress sweep, which should have been in the proportional (positive) direction. The Critical Tip Opening Displacement (CTOD) and Binder Yield Energy Test (BYET) appear to be the strongest test methods to identify potential for fatigue cracking in modified and unmodified asphalts given the largest rank order when compared to lab-scale fatigue and full-scale cracking.

An important advantage of the full-scale accelerated aging is that it essentially doubled the number of data points available to compare the ranking of in-situ binder properties and full-scale fatigue cracking. Work continues on this aspect.

Table 5: Strength of binder test methods to discriminate fatigue cracking performance.

Binder Test Method	Kendall's Tau Rank Order (Kendall and Gibbons 1996)	
	Lab-Scale Fatigue (Kutay et al. 2008)	Full Scale ALF Fatigue Cracking
Superpave Loss Modulus $|G^*| \times \sin\delta$	-0.8	-0.6
Time Sweep (Martono and Bahia 2008)	+0.6	+0.8
Stress Sweep (Martono and Bahia 2008)	-0.6	-0.4
Time Sweep Surrogate, High-Strain Loss Modulus (Shenoy 2002)	-0.6	-0.4
Critical Tip Opening Displacement, CTOD (Bodley et al. 2007, Andriescu et al. 2009)	+0.8	+1.0
Binder Yield Energy Test, BYET (Johnson et al. 2009)	+1.0	+0.8

5 SUMMARY AND CONCLUSIONS

The fatigue performance of HMA pavements with unmodified and modified asphalts was evaluated using accelerated pavement testing in early-aged and accelerated-aged conditions. Early-aged testing was conducted after about 11 months of natural exposure while the aged conditions were tested after a little more than five years of natural exposure plus eight weeks of full-scale accelerated aging at 74$^{\text{o}}$C. The aging process significantly decreased the fatigue performance and the overall ranking of the fatigue performance was the same before and after aging. The exceptions were the Arizona crumb rubber mixture, which was significantly impacted by the aging process and the reacted terpolymer mix was nearly un-affected.

The aging process triggered a different type of fatigue crack propagation. Early-aged fatigue cracking all progressed from the bottom to the top. The aged sections exhibited a mixture of top-down and bottom-up fatigue cracking, but the majority was top-down.

The dynamic modulus $|E^*|$ of the in-situ HMA was characterized before and after accelerated aging using indirect tension testing (IDT) methodology. The largest difference in modulus was seen between the upper layers and the bottom layers. The upper layers were stiffer despite having less density likely due to the aging and embrittlement. The IDT $|E^*|$ data indicate that the largest increase in mixture stiffness was due to more than five years of

natural exposure while the accelerate-aging process did not appear to cause a measurable increase in stiffness.

Extracted binder stiffness was characterized from the upper 25 mm of HMA and was sensitive enough to show increases in stiffness for both the natural exposure and accelerated aging. The aging process was more severe based on changes in the intermediate temperature properties than the high temperature properties. Natural exposure aging was found to be equivalent to more than the standard 20 hours in the Pressure Aging Vessel. Research continues to extract additional binder from all accelerated-aged lanes so the candidate parameters poised to replace the Superpave fatigue cracking specification will be compared back to the accelerated-aged performance in addition to the early-aged fatigue cracking performance.

REFERENCES

Airey, G., 2003, *State of the Art Report on Ageing Test Methods for Bituminous Pavement Material*, International Journal of Pavement Engineering, Vol.4, No.3, by Taylor and Francis Ltd.

Andriescu, A., N. Gibson, J. Youtcheff, X. Qi, S. Hesp, 2009, *Critical Crack Tip Opening Displacement as a Fatigue Cracking Criterion for Asphalt Mixtures*, Proceedings of Sixth International Conference on Maintenance and Rehabilitation of Pavements and Technological Control, Torino, Italy.

Bahia, H.U., D.I. Hanson, M. Zheng, H. Zhai, M. A. Khatri and R.M. Anderson, 2001, *Characterization of Modified Asphalt Binders in Superpave Mix Design*, NCHRP Report 459, Transportation Research Board – National Research Council, National Academy Press, Washington, D.C.

Bodley, T., A. Andriescu, S. Hesp, K. Tam, 2007, *Comparison between Binder and Hot Mix Asphalt Properties and Early Top-Down Wheel Path Cracking in a Northern Ontario Pavement Trial*, Asphalt Paving Technology, Journal of the Association of Asphalt Paving Technologists, Vol. 76.

Johnson, C., H. Wen and Hussain Bahia, 2009, *Practical Application of Viscoelastic Continuum Damage Theory to Asphalt Binder Fatigue Characterization,* Asphalt Paving Technology, Journal of the Association of Asphalt Paving Technologists, Vol. 78.

Kendall, M. and J. Gibbons, 1996, *Rank Correlation Methods*, Fifth edition, Oxford University Press.

Kim, Y.R., Y. Seo, M. King and M. Momen, 2004, *Dynamic Modulus Testing of Asphalt Concrete in Indirect Tension Mode*, Transportation Research Record: Journal of the Transportation Research Board, Volume 1891.

Kutay, M. E., N. Gibson and J. Youtcheff, 2008, *Conventional and Viscoelastic Continuum Damage (VECD) Based Fatigue Analysis of Polymer Modified Asphalt Pavements*, Asphalt Paving Technology, Journal of the Association of Asphalt Paving Technologists, Vol. 77.

Martono, W. and H. Bahia, 2008, *Developing a Surrogate Test for Fatigue of Asphalt Binders*, 87th Annual TRB Meeting Compendium of Papers DVD, Transportation Research Board – National Research Council, Washington, D.C.

Shenoy, A., 2002, *Fatigue Testing and Evaluation of Asphalt Binders Using the Dynamic Shear Rheometer,* ASTM Journal of Testing and Evaluation, Vol. 30, No. 4.